

## **COST-STSM-TD1301-27494 Scientific Report**

**STSM Topic: Development of compressive sensing techniques for medical applications of microwave imaging**

**STSM Applicant: Marija Stevanovic, School of Electrical Engineering, University of Belgrade, Serbia**

**Host: Dr. Lorenzo Crocco, Institute for the Electromagnetic Sensing of the Environment CNR - National Research Council, Naples (IT), crocco.l@irea.cnr.it**

**Period: 22.6.-7.7.2015.**

### **(i) Abstract**

During this STSM, we considered the application of the compressive sensing in the microwave imaging for brain stroke monitoring. In order to detect the progress of a stroke, we used data from several measurements separated in time. The differences in the measured electromagnetic field, indicate the changes in the electromagnetic properties of the brain due to the stroke. Since these changes are small and confined to a small region, compressive sensing yields accurate images with high resolution.

In this preliminary analysis, we utilized a numerical inhomogeneous head model. For simplicity, we assumed a two-dimensional (2D) geometry and the transverse-magnetic (TM) polarization. We compared the cases in which the prior knowledge of the electromagnetic parameters of the head was complete and only partial.

### **(ii) Purpose of the STSM**

The purpose of the STSM was to develop a close collaboration between the researchers from the host institution (Institute for the Electromagnetic Sensing of the Environment CNR - National Research Council, Naples, Italy) and the home institution (School of Electrical Engineering, University of Belgrade, Serbia). By visiting facilities of the IREA laboratory, meeting with people and learning about their research, we set up the initial stage of the future partnership. More important, during the second week of the visit, we have formulated the sparse imaging approach

and implemented it to the two-dimensional brain-stroke monitoring problem. As a future plan, we will generalize this model to the three-dimensional case.

### (iii) Description of the work carried out during the STSM

#### Electromagnetic Modeling

We consider the following scenario, consisting of a circular array of the electromagnetic sensors placed around the head. To reduce the reflection from the head, the sensors are placed in a coupling medium. In 2D geometry, the sensors are infinitely long probes. We assume that the sensors are excited one at a time by a unit electric current. Every sensor in the array measures the total electromagnetic field, perturbed by the presence of the head. By means of the volume equivalent principle, one may write

$$E_s(\mathbf{r}_j, \mathbf{r}_i) = j\omega \int_S (\varepsilon(\mathbf{r}') - \varepsilon_b(\mathbf{r}')) E_{\text{tot}}(\mathbf{r}', \mathbf{r}_i) G(\mathbf{r}_j, \mathbf{r}') dS', \quad (1)$$

$$E_s(\mathbf{r}_j, \mathbf{r}_i) = E_{\text{tot}}(\mathbf{r}_j, \mathbf{r}_i) - E_{\text{inc}}(\mathbf{r}_j, \mathbf{r}_i), \quad (2)$$

where  $E_s$  is the scattered electric field,  $E_{\text{tot}}$  is the total electric field,  $E_{\text{inc}}$  is the incident electric field (i.e., the field measured in the absence of the head),  $G$  is the Green's function,  $\mathbf{r}_i$  is the location of the transmitting antenna,  $\mathbf{r}_j$  is the location of the receiving antenna, and  $\mathbf{r}'$  is the position vector of the source point. Further,  $\varepsilon_b$  is the permittivity of coupling medium,  $\varepsilon$  is the permittivity of the head,  $\omega$  is the angular frequency and  $S$  is the cross-sectional area of the head.

In general, the reconstruction of the electromagnetic properties of the whole head from the electromagnetic measurements is a difficult task to the nonlinearity of the problem. However, we may linearize the problem with respect to the small differences in the electromagnetic properties occurring due to the stroke. By subtracting the electric field taken at a time instant  $t_1$  from the electric field taken at time instant  $t_2$ , we obtain the **differential** scattered field

$$\Delta E_s(\mathbf{r}_j, \mathbf{r}_i) = E_s(\mathbf{r}_j, \mathbf{r}_i; t_2) - E_s(\mathbf{r}_j, \mathbf{r}_i; t_1) = E_{\text{tot}}(\mathbf{r}_j, \mathbf{r}_i; t_2) - E_{\text{tot}}(\mathbf{r}_j, \mathbf{r}_i; t_1). \quad (3)$$

Assuming small changes,  $E_{\text{tot}}(\mathbf{r}', \mathbf{r}_i; t_1) \approx E_{\text{tot}}(\mathbf{r}', \mathbf{r}_i; t_2)$ . Hence, the differential scattered field is approximately

$$\Delta E_s(\mathbf{r}_j, \mathbf{r}_i) \approx j\omega \int_S \Delta \varepsilon(\mathbf{r}') E_{\text{tot}}(\mathbf{r}', \mathbf{r}_i; t_1) G(\mathbf{r}_j, \mathbf{r}') dS', \quad (4)$$

$$\Delta\varepsilon(\mathbf{r}') = \varepsilon(\mathbf{r}', t_2) - \varepsilon(\mathbf{r}', t_1), \quad (5)$$

where  $\Delta\varepsilon(\mathbf{r}')$  is the difference in the relative permittivity of the brain due to the presence of the stroke (i.e., the target). In the case when the stroke occupies only a small portion of the head, (4) becomes approximately

$$\Delta E_s(\mathbf{r}_j, \mathbf{r}_i) \approx j\omega\Delta\varepsilon(\mathbf{t}_s)E_{\text{tot}}(\mathbf{t}_s, \mathbf{r}_i)G(\mathbf{r}_j, \mathbf{t}_s)\Delta S, \quad (6)$$

where  $\mathbf{t}_s$  is the position-vector of the stroke and  $\Delta S$  is the stroke's cross-sectional area. Due to reciprocity, (6) is equivalent to

$$\Delta E_s(\mathbf{r}_j, \mathbf{r}_i) = j\omega\Delta\varepsilon E_{\text{tot}}(\mathbf{t}_s, \mathbf{r}_i)G(\mathbf{t}_s, \mathbf{r}_j)\Delta S. \quad (7)$$

We compute the Green's functions numerically, using the unit filament currents for the excitation. In this case, the Green's function is numerically equal to the total field, i.e.,

$$G(\mathbf{t}, \mathbf{r}_j) = E_{\text{tot}}(\mathbf{t}, \mathbf{r}_j)/I_j, \quad I_j = 1 \text{ A}. \quad (8)$$

Hence,

$$\Delta E_s(\mathbf{r}_j, \mathbf{r}_i; \mathbf{t}_s) = j\omega\Delta\varepsilon E_{\text{tot}}(\mathbf{t}_s, \mathbf{r}_i)E_{\text{tot}}(\mathbf{t}_s, \mathbf{r}_j)\Delta S. \quad (9)$$

## Sparse Processing

Since the location of the scatterer is unknown, we divide the interior of the brain into a uniform grid. Each node in the grid represents the potential location of the stroke. The measurement model, when the  $i$ th sensor is transmitting, reads

$$\begin{bmatrix} \Delta E_s(\mathbf{r}_1, \mathbf{r}_i) \\ \vdots \\ \Delta E_s(\mathbf{r}_M, \mathbf{r}_i) \end{bmatrix} = \begin{bmatrix} E_{\text{tot}}(\mathbf{t}_1, \mathbf{r}_i)E_{\text{tot}}(\mathbf{t}_1, \mathbf{r}_i) & \dots & E_{\text{tot}}(\mathbf{t}_L, \mathbf{r}_i)E_{\text{tot}}(\mathbf{t}_L, \mathbf{r}_i) \\ \vdots & \ddots & \vdots \\ E_{\text{tot}}(\mathbf{t}_1, \mathbf{r}_M)E_{\text{tot}}(\mathbf{t}_1, \mathbf{r}_i) & \dots & E_{\text{tot}}(\mathbf{t}_L, \mathbf{r}_M)E_{\text{tot}}(\mathbf{t}_L, \mathbf{r}_i) \end{bmatrix} \begin{bmatrix} \tau_1 \\ \vdots \\ \tau_L \end{bmatrix}, \quad \tau_l = j\omega\Delta\varepsilon_l\Delta S, \quad (10)$$

where  $\Delta\varepsilon_l$  is the differential permittivity of  $l$ th scatterer and  $L$  is the size of the grid. In the matrix form (10) is

$$\mathbf{e}_s(\mathbf{r}_i) = \mathbf{H}(\mathbf{r}_i)\boldsymbol{\tau}. \quad (11)$$

In the sparse processing framework, only a few elements of the vector  $\boldsymbol{\tau}$  have significant values. Therefore, we impose the sparsity constraint to solve the problem. The minimization function reads

$$\hat{\boldsymbol{\tau}} = \min_{\boldsymbol{\tau}} \left\{ \|\mathbf{e}_s(\mathbf{r}_i) - \mathbf{H}(\mathbf{r}_i)\boldsymbol{\tau}\|_2^2 + \gamma \|\boldsymbol{\tau}\|_1 \right\}, \quad (12)$$

where  $\gamma$  is the regularization coefficient. Nevertheless, the sparse model (10)-(12), emphasizes the grid points close to the boundary of the head where the values of the Green's functions are the largest. Therefore, we normalize the elements of the system matrix

$$\tilde{\mathbf{H}}(\mathbf{r}_i) = \begin{bmatrix} \frac{E_{\text{tot}}(\mathbf{t}_1, \mathbf{r}_1)E_{\text{tot}}(\mathbf{t}_1, \mathbf{r}_i)}{|E_{\text{tot}}(\mathbf{t}_1, \mathbf{r}_1)E_{\text{tot}}(\mathbf{t}_1, \mathbf{r}_i)|} & \cdots & \frac{E_{\text{tot}}(\mathbf{t}_L, \mathbf{r}_1)E_{\text{tot}}(\mathbf{t}_L, \mathbf{r}_i)}{|E_{\text{tot}}(\mathbf{t}_L, \mathbf{r}_1)E_{\text{tot}}(\mathbf{t}_L, \mathbf{r}_i)|} \\ \vdots & \ddots & \vdots \\ \frac{E_{\text{tot}}(\mathbf{t}_1, \mathbf{r}_M)E_{\text{tot}}(\mathbf{t}_1, \mathbf{r}_i)}{|E_{\text{tot}}(\mathbf{t}_1, \mathbf{r}_M)E_{\text{tot}}(\mathbf{t}_1, \mathbf{r}_i)|} & \cdots & \frac{E_{\text{tot}}(\mathbf{t}_L, \mathbf{r}_M)E_{\text{tot}}(\mathbf{t}_L, \mathbf{r}_i)}{|E_{\text{tot}}(\mathbf{t}_L, \mathbf{r}_M)E_{\text{tot}}(\mathbf{t}_L, \mathbf{r}_i)|} \end{bmatrix}. \quad (12)$$

The new measurement model reads

$$\mathbf{e}_s(\mathbf{r}_i) = \tilde{\mathbf{H}}(\mathbf{r}_i)\tilde{\boldsymbol{\tau}}, \quad (13)$$

However, the solution vector is not anymore proportional to the permittivity difference.

## Joint Processing of Several Incident Angles

In order to remove the artifacts due to the noise or errors in the measurement positions, we combine the measurements corresponding to different transmissions. The joint measurement model when all incident angles are simultaneously used is

$$\begin{bmatrix} \mathbf{e}_s(\mathbf{r}_1) \\ \vdots \\ \mathbf{e}_s(\mathbf{r}_M) \end{bmatrix} = \begin{bmatrix} \tilde{\mathbf{H}}(\mathbf{r}_1) \\ \vdots \\ \tilde{\mathbf{H}}(\mathbf{r}_M) \end{bmatrix} \tilde{\boldsymbol{\tau}}. \quad (14)$$

Nevertheless, we have also investigated various combinations of the transmitters and the receivers.

## Numerical Results

We have simulated the follow up of a hemorrhagic stroke. We have considered the phantom corresponding to slice 45 of the Zubal phantom, as shown in Fig. 1. We modeled the stroke as an elliptic inclusion with the electromagnetic parameters the same as those of the blood at 1 GHz ( $\epsilon_r = 61.1, \sigma = 1.6 S/m$ ). The dimensions of the stroke at times  $t_2$  and  $t_1$  were, respectively,  $a_2 = 2$  cm and  $b_2 = 4$  cm,  $a_1 = 0.5$  cm and  $b_1 = 1$  cm, where  $a$  and  $b$  stand for the semi-minor and semi-major axis, respectively.

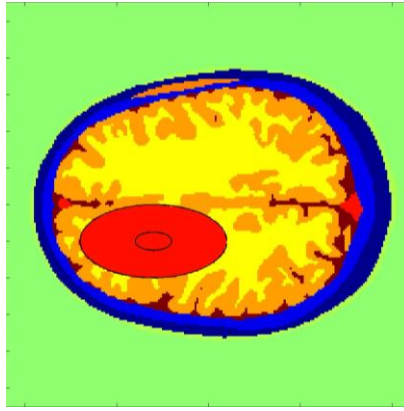


Fig. 1. The head model and the elliptic inclusions simulating the stroke at two different moments.

In the simulations, the differential data have been gathered using 32 infinite length filamentary antennas oriented along the  $z$ -axis. Sources and measurement points are evenly spaced on a circumference having radius  $r = 18$  cm surrounding the investigated domain, that is, a square of side 22 cm.

### Scenario 1 - Ideal Case

As a benchmark, we considered an ideal case in which the data were noiseless and the prior knowledge about the electromagnetic parameters of the head (apart from the stroke) was perfect. Hence, we computed the Green's functions using the exact electromagnetic parameters of the head.

The measurements were taken by the circular array of  $M$  elements, where each element in the array worked both as the transmitter and the receiver. However, in the sparse processing we did not use all available data simultaneously. Instead, we considered different "views", where each view corresponded to the transmissions of  $N_s$  adjacent antenna elements. For the received signals, we used data from all  $M$  antennas. Hence, for each view, the size of the system matrix was  $N_s M \times L$ . To obtain the whole image of the target we changed the view for the angle subtended by  $\Delta$  array elements. Equivalently, the system may be represented by a rotating transmitting array of  $N_s$  elements and a receiving array of  $M$  elements.

In the first row of Fig. 2, we show the results obtained for several dimensions of the transmitting array,  $N_s$ . The rotation of the transmitting array corresponded to  $\Delta = N_s$  elements. In the second row, we show the effect of scaling in which more weight is given to the pixels away from the head boundary.

As the number of the elements in the transmitting array increases, or equivalently, by processing data obtained from a wider angle, the estimate improves. Also, the scaling of the obtained image reveals the pixels in the interior. As a comparison, Fig. 3 shows the results for  $\Delta = 2$ . Due to larger number of views, the additional pixels in the interior of the target have appeared.

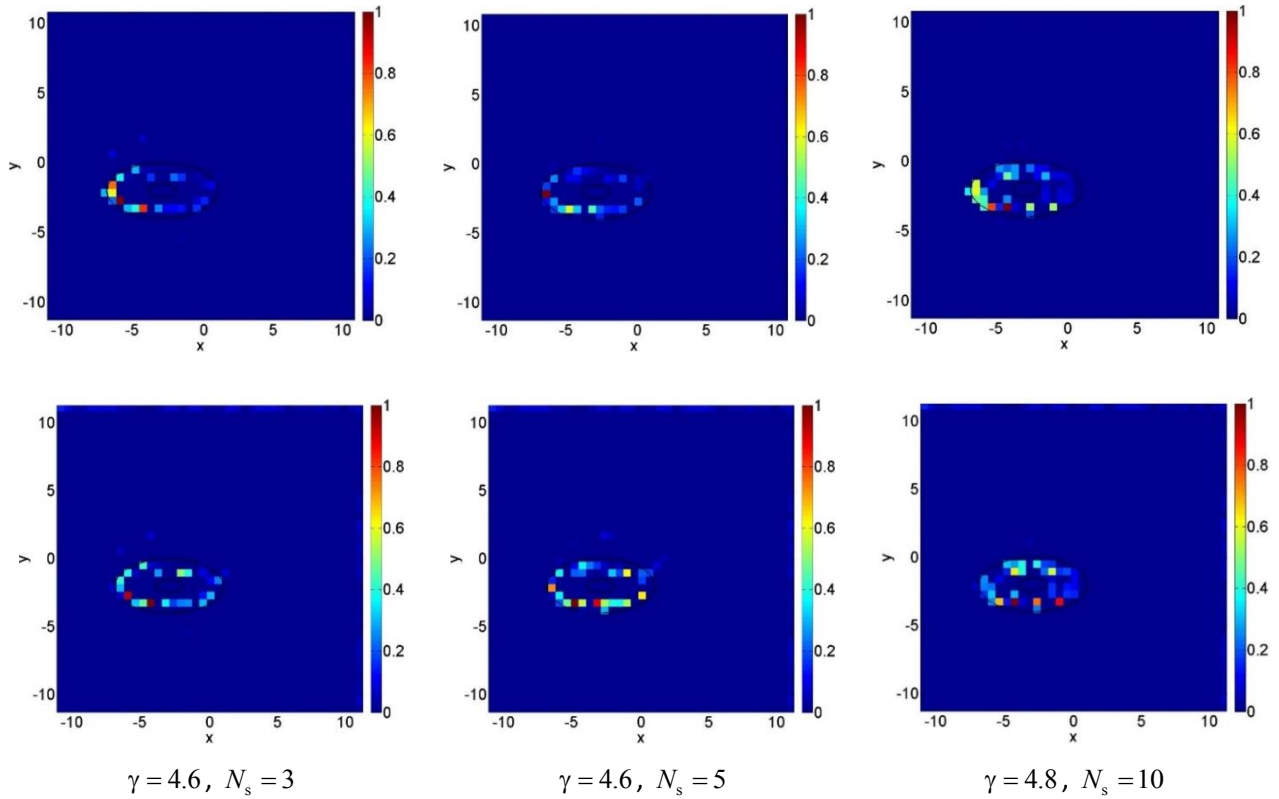


Fig. 2. The sparse processing results obtained for different sizes of the transmitting arrays and  $\Delta = N_s$ . The images in the second row are obtained by postprocessing of the images of the first row, where more weight are given to the pixels in the head interior.

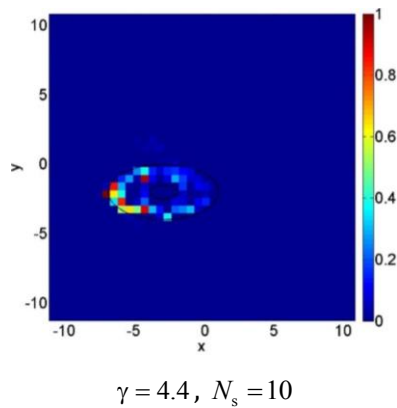


Fig. 3. The sparse processing results obtained for  $N_s = 10$  and  $\Delta = 2$ .

## Scenario 2 - Ideal Case with the Complementary Transmit-Receive Arrays

The experiment set up was the same as in the previous case, with the exception of the receiving array. As before, we used jointly the data obtained from  $N_s$  transmissions. However, for the received signals, we used the *complementary* part of the array consisting of  $M - N_s$  array elements. Hence, the size of the system matrix is  $(M - N_s)N_sL$ . The corresponding measurement model reads

$$\mathbf{e}_s = \tilde{\mathbf{H}}\tilde{\boldsymbol{\tau}}, \quad (10)$$

$$\begin{bmatrix} \mathbf{e}_s(\mathbf{r}_{n_1}) \\ \vdots \\ \mathbf{e}_s(\mathbf{r}_{n_2}) \end{bmatrix} = \begin{bmatrix} \tilde{\mathbf{H}}(\mathbf{r}_{n_1}) \\ \vdots \\ \tilde{\mathbf{H}}(\mathbf{r}_{n_2}) \end{bmatrix} \tilde{\boldsymbol{\tau}}, \quad (11)$$

$$\tilde{\mathbf{H}}(\mathbf{r}_i) = \begin{bmatrix} \frac{E_{\text{tot}}(\mathbf{t}_1, \mathbf{r}_{m_1})E_{\text{tot}}(\mathbf{t}_1, \mathbf{r}_i)}{|E_{\text{tot}}(\mathbf{t}_1, \mathbf{r}_{m_1})E_{\text{tot}}(\mathbf{t}_1, \mathbf{r}_i)|} & \cdots & \frac{E_{\text{tot}}(\mathbf{t}_L, \mathbf{r}_{m_1})E_{\text{tot}}(\mathbf{t}_L, \mathbf{r}_i)}{|E_{\text{tot}}(\mathbf{t}_L, \mathbf{r}_{m_1})E_{\text{tot}}(\mathbf{t}_L, \mathbf{r}_i)|} \\ \vdots & \ddots & \vdots \\ \frac{E_{\text{tot}}(\mathbf{t}_1, \mathbf{r}_{m_2})E_{\text{tot}}(\mathbf{t}_1, \mathbf{r}_i)}{|E_{\text{tot}}(\mathbf{t}_1, \mathbf{r}_{m_2})E_{\text{tot}}(\mathbf{t}_1, \mathbf{r}_i)|} & \cdots & \frac{E_{\text{tot}}(\mathbf{t}_L, \mathbf{r}_{m_2})E_{\text{tot}}(\mathbf{t}_L, \mathbf{r}_i)}{|E_{\text{tot}}(\mathbf{t}_L, \mathbf{r}_{m_2})E_{\text{tot}}(\mathbf{t}_L, \mathbf{r}_i)|} \end{bmatrix}, \quad (12)$$

Where  $m_1$  and  $m_2$  are the indices of the first and the last transmitter, respectively. Similarly,  $n_1$  and  $n_2$  are the indices of the first and the last receiver respectively. To obtain the complete image of the target, we rotated the transmission array as described in the previous section. The first element in the transmit array was shifted for  $\Delta = N_s$  elements. Fig. 4 presents the scaled results for different values of  $N_s$ . As in the previous scenario, the estimated pixels were properly located in the area between two ellipses, giving the right estimated of the stroke progress. The image becomes more refined for wider view angles.

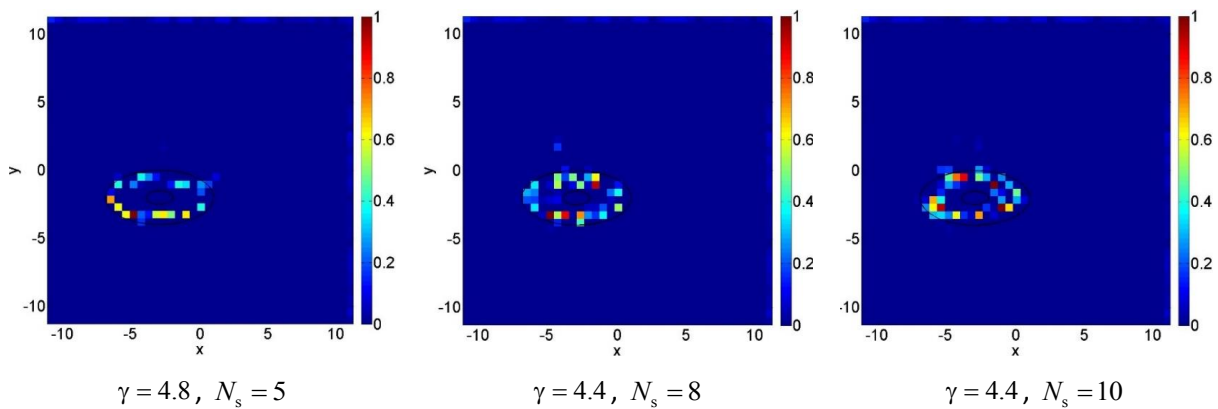


Fig. 4. The sparse processing results obtained for different sizes of the transmitting arrays and  $\Delta = N_s$ .

### Scenario 3 –Realistic Case

By applying the additive Gaussian noise, we corrupted the simulation data. We computed the signal to noise ratio ( $SNR$ ) with the respect to the power of the scattered data. In our computations, we set  $SNR=10$  dB. In addition, we computed the Green's function using the average instead of the exact head model. The transmitting arrays consisted of  $N_s$  antennas and the receiving array consisted of all  $M$  antennas. In Fig. 3, we show the results obtained for several choices of  $N_s$ . In the creation of the image, we used different views obtained by rotating the transmitting array for  $\Delta=2$ .

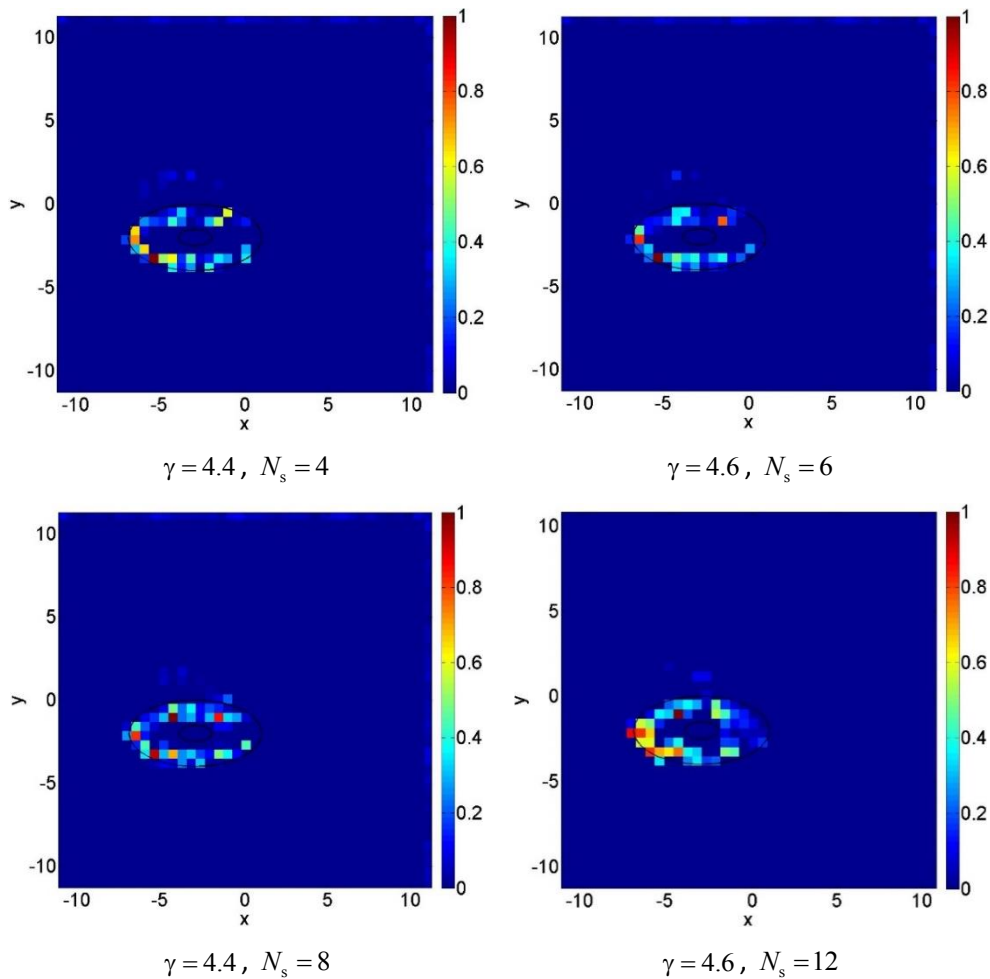
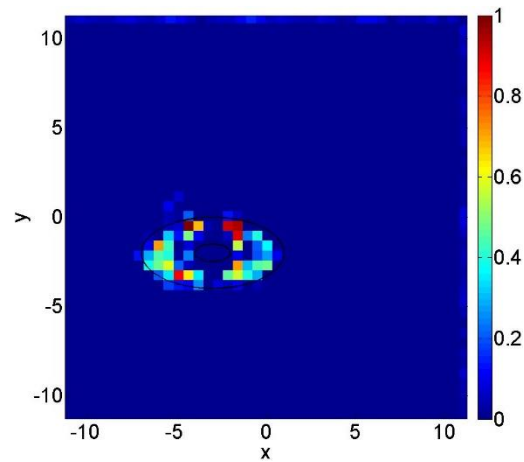


Fig. 5. The sparse processing results obtained for different sizes of the transmitting arrays and  $\Delta=2$ . The images were normalized.

For a comparison, Fig. 6 shows the results obtained with complementary receiving array for  $N_s=12$  and  $\Delta=2$ .





$$\gamma = 4.6, N_s = 12$$

Fig. 6. The sparse processing results obtained for  $N_s = 12$  and  $\Delta = 2$ . The image was normalized.

#### **(iv) Description of the main results obtained**

During this STSM, we investigated the application of the sparse processing framework to the differential microwave imaging of the brain. We studied different array configurations and post-processing techniques. Moreover, we considered a realistic case in which the data were corrupted by the noise, and the knowledge of the electromagnetic parameters of the head was very limited (average head model). The obtained results were promising and represent the strong foundation for a future work.

#### **(v) Future collaboration with host institution (if applicable)**

During this visit, we agreed to continue our collaboration by considering more realistic scenarios (three-dimensional geometry, measurement position errors, etc.). Besides brain imaging, which is of primary interest, we plan to implement our algorithms in other microwave imaging problems in which compressive sensing can be successfully applied.

#### **(vi) Foreseen publications/articles resulting or to result from the STSM (if applicable)**

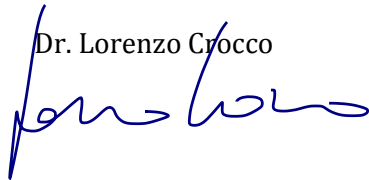
Our goal is to submit the results obtained during STSM to the EUCAP conference. However, the main plan is to extend the analysis in order to be suitable for a journal publication.

#### **(vii) Confirmation of the host of the successful execution of the STSM**

I confirm that Marija Stevanovic from School of Electrical Engineering, University of Belgrade worked in our laboratories at Institute for the Electromagnetic Sensing of the Environment CNR - National Research Council from 22.6 to 7.7.2015.

The visit has been successful and the results are described in this report, which I confirm.

Dr. Lorenzo Crocco



Naples 01.08.15



istituto per il rilevamento  
elettromagnetico  
dell'ambiente